The Journal of Neuroscience, October 1, 1999, *19*(19):8337–8348

δ Opioid Receptor Modulation of Several Voltage-Dependent Ca^{2+} Currents in Rat Sensory Neurons

Cristian G. Acosta and Héctor S. López

Instituto de Investigación Médica Mercedes y Martín Ferreyra, Consejo Nacional de Investigaciones Científicas y Técnicas, 5000 Córdoba, Argentina

Endogenous enkephalins and δ opiates affect sensory function and pain sensation by inhibiting synaptic transmission in sensory circuits via delta opioid receptors (DORs). DORs have long been suspected of mediating these effects by modulating voltage-dependent Ca^{2+} entry in primary sensory neurons. However, not only has this hypothesis never been validated in these cells, but in fact several previous studies have only turned up negative results. By using whole-cell current recordings, we show that the δ enkephalin analog [D-Ala^2, D-Leu^5]-enkephalin (DADLE) inhibits, via DORs, L-, N-, P-, and Q-high voltage-activated Ca^{2+} channel currents in cultured rat dorsal root ganglion (DRG) neurons. The percentage of responding cells was remarkably high (75%) within a novel subpopulation of substance P-containing neurons compared with the other cells (18–35%). DADLE (1 μM) inhibited 32% of the total barium current through calcium channels (I_{Ba}). A δ (naltrindole, 1 μM), but not a μ (β-funaltrexamine, 5 μM), antagonist prevented the DADLE response, whereas a DOR-2 subtype (deltorphin-II, 100 nM), but not a DOR-1 (DPDPE, 1 μM), agonist mimicked the response. L-, N-, P-, and Q-type currents contributed, on average, 18, 48, 14, and 16% to the total I_{Ba} and 19, 50, 26, and 20% to the DADLE-sensitive current, respectively. The drug-insensitive R-type current component was not affected by the agonist. This work represents the first demonstration that DORs modulate Ca^{2+} entry in sensory neurons and suggests that δ opioids could affect diverse Ca^{2+}-dependent processes linked to Ca^{2+} influx through different high-voltage-activated channel types.

Key words: Ca^{2+} channel; δ opioid receptor; modulation; sensory neuron; dorsal root ganglion; high-voltage-activated Ca^{2+} current; nimodipine; ω-conotoxin GVIA; ω-agatoxin IVA; ω-conotoxin MVIIC

Delta opioid receptors (DORs) and their endogenous ligands Met-enkephalin and Leu-enkephalin have widespread and matching distributions in spinal cord pain-related primary sensory circuits of the rat, mouse, cat, and monkey in which they modulate the transmission of afferent nociceptive neural activity (Aronin et al., 1981; Dickenson et al., 1987; Miller and Seybold, 1989; Ramabandran et al., 1990; Levine et al., 1993; Standifer et al., 1994; Narita and Tseng, 1995). Despite much progress, the cellular mechanism mediating DOR-induced modulation of neural transmission in sensory neurons remains to be clarified. Ever since the demonstration of enkephalin-induced inhibition of substance P release in sensory synapses (Jessell and Iversen, 1977), later shown to involve DORs (Collin et al., 1991), the dominant hypothesis has been that DORs inhibit Ca^{2+} influx to sensory neurons and, consequently, Ca^{2+}-dependent transmitter release.

Several lines of evidence lend credence to the hypothesis of DOR-induced inhibition of Ca^{2+} influx. First, sensory neurons express DORs (Ji et al., 1995) and an assortment of high-voltage-activated Ca^{2+} channels (HVACC) (Mintz et al., 1992; Cardenas et al., 1995; Rusin and Moises, 1995). Second, DOR activation by enkephalins presynaptically inhibits the transmission of pain-related activity in the spinal cord (Dickenson et al., 1987; Glaum et al., 1994) and brain (Wang et al., 1996), as well as the pain-induced release of substance P (Zachariou and Goldstein, 1996). Third, DORs localize in presynaptic terminals of spinal cord-projecting sensory neurons (Cheng et al., 1995; van Bockstaele et al., 1997). Fourth, DORs inhibit HVACC currents in secretory (Albillos et al., 1996; Piros et al., 1996) and neuronal cell lines (Hescheler et al., 1987; McFadzean and Docherty, 1989; Toselli et al., 1997).

Indirect data suggested that DOR might inhibit Ca^{2+} inward currents in sensory neurons as well (Shen and Crain, 1989). However, more recent studies in those cells yielded negative results (Schroeder et al., 1991; Liu et al., 1995). In this study, we reexamined this question and show that an enkephalin analog that acts on both pharmacological DOR subtypes (DORs-1 and DORs-2) (Reisine, 1995) consistently inhibited the HVACC current in all subpopulations of postnatal rat sensory neurons in culture. The low overall frequency of responding cells and the involvement of a previously untested DOR subtype (DOR-2) may explain previous negative results (Schroeder et al., 1991; Liu et al., 1995).

DORs targeted L, N, P, and Q HVACC current types as defined by their sensitivity to nimodipine, ω-conotoxin-GVIA (ω-CTx-GVIA), ω-agatoxin-IVA (ω-Aga-IVA), and ω-conotoxin-MVIIC (ω-CTx-MVIIC), respectively (Llinás et al., 1989; Mintz et al., 1992; Randall and Tsien, 1995; McDonough et al., 1996). The inhibition of the HVACC current types mediating transmitter release (N, P, and Q) in primary sensory affer-

Received Feb. 18, 1999; revised July 16, 1999; accepted July 22, 1999.

This work was supported by International Foundation for Science Grant F/2632-1, Consejo de Investigaciones Cientificas y Tecnológicas de Córdoba Grant 4052, and Fondo Nacional para las Ciencias y la Tecnología Grant PICT 5-01202. H.L. is a career member of Consejo Nacional de Investigaciones Científicas y Técnicas (CONICET), and C.A. is the recipient of a fellowship from CONICET. We thank Dr. H. Carrer for useful comments on the manuscript, Dr. A. Cáceres for help with the image analysis equipment and the gift of some reagents, and A. Fábrega for conducting some experiments.

Correspondence should be addressed to Héctor S. López, Instituto de Investigación Médica Mercedes y Martín Ferreyra, Casilla de Corrcos 389, 5000 Córdoba, Argentina. E-mail: hlopez@immf.uncor.edu.

 0270-6474/99/198337-12$05.00/0

ents (Yu et al., 1992; Gruner and Silva, 1994) and brain (Reuter, 1996) validates the hypothesis that DORs may control synaptic transmission by reducing Ca^{2+} influx. In addition, the data suggest a broad influence of DORs in Ca^{2+}-dependent cellular processes linked to specific HVACC, such as sensory neuron development and survival and gene expression (Finkbeiner and Greenberg, 1996; Reuter, 1996; Hardingham et al., 1997).

MATERIALS AND METHODS

Cell culture and immunocytochemistry. All procedures were in strict accordance with the Guide for the Care and Use of Laboratory Animals, in agreement with the Society for Neuroscience Policy. Dorsal root ganglia (DRG) from the cephalic, thoracic, and lumbar regions were obtained from 5- to 11-d-old neonatal Sprague Dawley rats of either sex, decapitated under ether deep anesthesia, and kept at 4°C in HBSS until dissociated by enzymatic digestion with 0.25% trypsin and 0.5% collagenase for 30 min at 37°C, followed by gentle mechanical trituration using a fire-polished Pasteur pipette. After addition of 2 ml of culture media containing 10% fetal bovine serum (MEM10) to halt the enzymatic activity, the cell suspension was centrifuged at 2000 rpm for 5 min. The supernatant was discarded, and the pellet was resuspended in MEM10. Then, further mechanical dissociation was performed using Pasteur pipettes of increasingly smaller tip diameters. Once dissociated, the neurons were plated on coverslips coated with 0.25% collagen and 0.05% poly-D-lysine and kept at 36°C in MEM10 for 1 hr. Then, additional media was added to reach a final volume of ~2 ml in each culture dish. The culture media was always supplemented with penicillin–streptomycin (200 IU per 200 μg/ml, respectively) to prevent bacterial–fungal contamination.

The cells were maintained in an incubator at 36°C and 4% CO_2 until used for electrophysiology. No nerve growth factor was added to the media because postnatal sensory neurons do not require it for survival (Ruit et al., 1992). To inhibit the proliferation of fibroblasts, 10 μM β-D-arabinofuranoside cytokine was added to the culture media 24 hr after plating and then every 48 hr. The culture media was replaced by 50% every 48 hr. The cultures consisted of a mixed population of neurons of varied sizes. Typically, the frequency of response to the agonist (inhibition of currents through Ca^{2+} channels) was low during the first 12 hr in culture, increased, and reached a peak and stabilized at 24 hr. Most recording experiments were done 12–48 hr after cell plating and always within 4 d in culture. Cells with no or minimal neurite development were used.

The immunocytochemistry experiments for labeling of substance P and α_{1C} subunits of L-type Ca^{2+} channels used low-density cultures, following established protocols (Cáceres et al., 1992). In brief, cells were fixed with paraformaldehyde–sucrose for 20 min, washed with PBS, permeabilized with 0.2% Triton X-100 for 5 min, washed three times for 5 min with PBS, and incubated overnight with either a rat monoclonal antibody against substance P, clone NC1/34 (diluted 1:20), or a rabbit polyclonal antibody against the α_{1C} subunit (diluted 1:100). The coverslips were incubated previously for 1 hr with 5% bovine serum albumin (BSA) to block nonspecific binding sites. An anti-rat IgG labeled with fit-C or an anti-rabbit IgG labeled with rhodamine were used as secondary antibodies in each case, with which the coverslips were incubated for 1 hr at room temperature. All antibodies were dissolved in 1% BSA. The procedure for immunodetection of α_{1C} subunits was performed at 4°C to avoid protease-mediated digestion (Hell et al., 1993). The coverslips were mounted on glass slides with FluorSave (Calbiochem, La Jolla, CA), and observed 24 hr later with a fluorescein filter in a epifluorescence microscope (Axiovert TM35; Zeiss, Oberkochen, Germany).

Electrophysiology and data analysis. Coverslips containing neurons were removed from the incubator and placed into the recording chamber just before starting the electrophysiological experiments. Ba^{2+} currents (I_{Ba}) flowing through HVACC were recorded at room temperature (20–23°C) using the whole-cell configuration of the patch-clamp technique (Hamill et al., 1981). The composition of the pipette solution was (in mM) 120 CsCl, 20 TEA-Cl, 5 Cl_2Mg, 10 EGTA, 10 HEPES, 4 Na_2ATP, 0.1 Li_2GTP, and 0.1 leupeptin, pH adjusted to 7.4 with CsOH. Two external solutions were used: a Tyrode's solution containing (in mM) 135 NaCl, 2.5 KCl, 4 $CaCl_2$, 2 $MgCl_2$, 10 D-glucose, and 10 HEPES, pH adjusted to 7.4 with NaOH; and a Ba^{2+}-containing solution, referred to as Ba-solution, containing (in mM) 5 $BaCl_2$, 150 *N*-methyl-D-glucamine, 2 $MgCl_2$, 10 D-glucose, and 10 HEPES, pH adjusted to 7.4 with HCl. The concentration of the charge carrier Ba^{2+} was limited to 5 mM because higher concentrations can significantly interfere with toxin binding to HVACC (McDonough et al., 1996).

The recordings were made with either an Axopatch 200A (Axon Instruments, Foster City, CA) or a List EPC-7 (Medical Systems, Greenvale, NY) amplifier. Data acquisition was controlled with a desktop computer equipped with an analog-to-digital converter (Scientific Solutions, Solon, OH). The currents were low-pass filtered at 2 kHz, sampled at least at 10 kHz, and recorded on hard disk. The recording pipettes were made from thin-walled capillary glass (inner diameter of 1.0 mm; catalog #7052; Garner Glass Company, Claremont, CA) using a horizontal puller (P-97; Sutter Instruments, Novato, CA) and fire-polished with a microforge (M-83; Narishige, Tokyo, Japan). When filled with internal solution, they had a resistance of 2–3 MΩ. The series resistance was compensated up to 70–95%. No corrections for liquid junction potentials were made. Leak currents were subtracted on-line using a P/4 routine. When removed from the incubator and first placed in the recording chamber, the cells were bathed with the Tyrode's solution and stayed in it until the whole-cell configuration was achieved. Then, the external solution was exchanged to the Ba-solution while holding the cell at −80 mV.

We required the data to meet three criteria to qualify for further analysis: (1) negligible I_{Ba} rundown over the entire duration of the experiment, (2) a fully reversible agonist response, and (3) current waveforms free from artifacts indicative of poor space clamp, such as "notches" or slow components in the decay of capacitive currents. Unless otherwise noted, agonist and drug effects on I_{Ba} were measured on current waveforms activated with 20–50 msec command pulses to 0 mV from a holding potential (V_H) of −70 mV or more positive and delivered every 15–30 sec. The effects of the different drugs on the HVACC currents were quantified off-line using custom-made software by measuring the current amplitude at the end of the depolarizing test pulses.

Pharmacology. A small-volume (100 μl) recording chamber was continuously perfused with control or drug-containing external solutions at an approximate rate of 0.6 ml/min using a system of multiple Teflon tubes connected to reservoirs containing the various solutions. All drugs were dissolved in the Ba-solution and were applied and removed by exchanging the external solution, which took ~15 sec. This relatively slow speed of solution exchange did not constitute an impediment because this work is not concerned with kinetic aspects. DORs were activated with the enkephalin analog [D-Ala^2, D-Leu^5]-enkephalin (DADLE) (1 μM), which nonselectively activates the DOR subtypes DORs-1 and DORs-2. [D-Pen^2, D-Pen^5]-enkephalin (DPDPE) (1 μM), and Tyr-D-Ala-Phe-Glu-Val-Gly-NH_2 (deltorphin-II) (100 nM) were used as DOR-1- and DOR-2-selective agonists, respectively. The δ-specific action of DADLE was tested with the highly selective DOR antagonist naltrindole (1 μM). Mu opioid receptors (MORs) were activated with the selective agonist Tyr-Pro-*N*-MePhe-D-Pro-NH_2 (PLO17) (1 μM). Opioid agonists and antagonists were reconstituted from stock lyophilized frozen (−20°C) aliquots the day of the experiment. In some cases, unused solutions were refrozen to be used in the following experiment without loss of pharmacological potency.

Ca^{2+} channel-blocking drugs were applied at concentrations or in combinations that optimally targeted specific types of HVACC (10 μM nimodipine, 2 μM ω-conotoxin GVIA, 50 nM ω-agatoxin IVA, and 0.5–1 μM ω-conotoxin MVIIC). We used two experimental protocols (protocol-1 and protocol-2) to estimate the contribution of a given pharmacological HVACC current type to I_{Ba} and to the DADLE-sensitive current (I_D). Protocol-1 tested the effect of DADLE on a specific HVACC current type, pharmacologically isolated by blocking all other current components with a mixture of drugs; a DADLE-induced inhibition of the isolated current indicated that it contributed to I_D. This protocol was used to estimate the contributions to I_D, as well as to I_{Ba}, of HVACC current types for which no selective blockers are available (Q- and R-types) and in addition to protocol-2 to gather complementary data on other current types. With protocol-1, the percentage contribution of a given HVACC current type to I_D was equal to [(magnitude of inhibition during second agonist application / magnitude of inhibition during first agonist application) × 100]. The tests for the contribution of Q-type current involved only one agonist application in the presence of Ca^{2+} channel blockers, and therefore the magnitude of the first inhibition was estimated from a separate, large number of cells. Protocol-2 measured the extent of agonist-induced I_{Ba} inhibition before and after the blockade

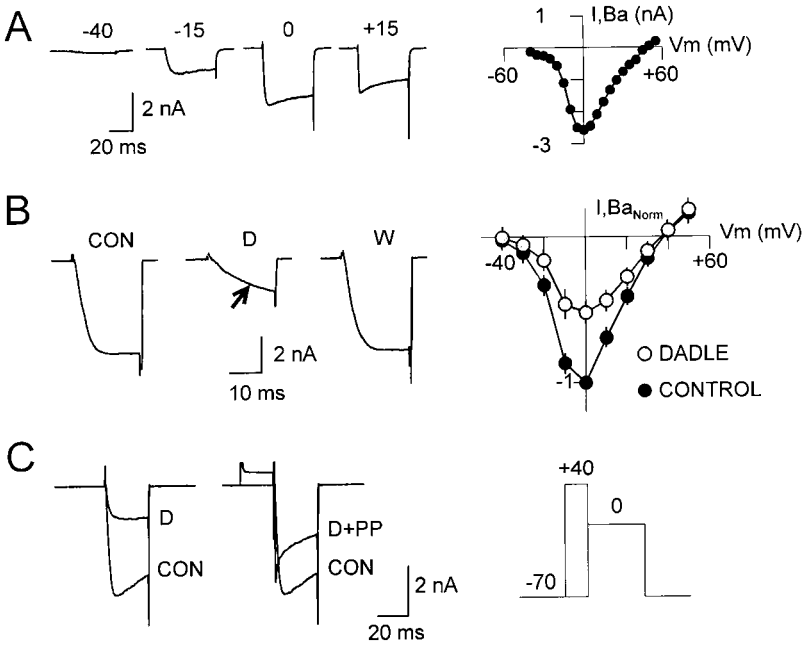

Figure 1. HVACC currents in cultured postnatal DRG neurons and characteristics of their inhibition by DADLE. *A*, Whole-cell Ba^{2+} current (I_{Ba}) evoked with 40 msec voltage pulses to −40, −15, 0, and 15 mV, from a V_H of −70 mV (*left*) and *I–V* plot of I_{Ba} at the end of 40 msec voltage test pulses (*right*). The voltage pulses, delivered every 15 sec, ranged from −40 to 55 mV, with 5 mV intervals, from a V_H of −70 mV. *B*, *Left* shows the preagonist control I_{Ba} current (*trace CON*) and its inhibition by 1 μM DADLE (*trace D*), obtained at 0 mV from a V_H of −70 mV. The agonist effect fully reversed upon agonist washout (*trace W*). The inhibited current typically showed a slowing down of activation (*arrow* in *trace D*). The *I–V* relationship (*right*) of the normalized I_{Ba} (data from 3 neurons) measured 25 msec after the onset of the test pulse, before (*filled circles*), and during (*hatched circles*) DADLE (1 μM) inhibition illustrates the current reduction in a wide range of test voltages (−40 to 50 mV). *C*, Voltage dependence of the agonist-mediated I_{Ba} inhibition. The inhibition of the control I_{Ba} current observed at 0 mV (*left panel, traces CON and D*) was partially removed by 20 msec prepulse to 40 mV, which preceded the test pulse to 0 mV (*right panel, trace D+PP*; for comparison, the preagonist control current was also included). The agonist was present throughout. The voltage pulse protocol is shown on the *right*. On average, the prepulse depolarization reverted 39% of the inhibition.

of a specific HVACC type; it was concluded that such current contributed to I_D if its suppression reduced or occluded the agonist-induced inhibition. This protocol was used to evaluate the contributions of N-, P-, and L-type HVACC currents to I_{Ba} and I_D because those currents can be selectively inhibited by ω-conotoxin GVIA, ω-agatoxin IVA, and nimodipine, respectively. With protocol-2, the percentage contribution of a given HVACC current type to I_D was equal to [(reduction of the current inhibition observed during second agonist application / magnitude of inhibition during first agonist application) × 100].

The contribution of only one type of HVACC current to I_D was tested in any given cell to limit agonist exposure to two applications: the first to obtain a control response, and the second to evaluate its reduction after the block of a specific HVACC current type. We chose this design because, in preliminary experiments, we found that I_{Ba} inhibition and recovery became progressively smaller and slower, respectively, with repeated DADLE applications, and these changes started to be noticeable with the third agonist application.

The opioid agonists DADLE, DPDPE, and PLO-17 were from Peninsula Labs (Belmont, CA). ω-CTx-GVIA, ω-Aga-IVA, ω-CTx-MVIIC, and the rabbit polyclonal antibody against α_{1C} subunits of L-type Ca^{2+} channels were from Alomone Labs (Jerusalem, Israel). Naltrindole, naloxone, and nimodipine were from Research Biochemicals (Natick, MA). The antibody against substance P was from Sera-Lab (Accurate Chemical & Scientific Corp., Westbury, NY). Stock solutions of ω-CTx-GVIA, ω-Aga-IVA, and ω-CTx-MVIIC were prepared in water and stored at −20°C for no longer than 1 month. Nimodipine was diluted in methanol (1:2500) and stored in a light-proof container at −20°C. These aliquots were dissolved in external solution the day of the experiment. The fit-C- and rhodamine-conjugated secondary antibodies and the rest of the reagents were from Sigma (St. Louis, MO). *S*-(±)-Bay-K 8644 was a gift of Dr. A. Hernández-Cruz (Instituto Fisiología Celular, Departamento Neurociencia, UNAM, M.F., México).

RESULTS

DOR-mediated inhibition of HVACC currents

Figure 1*A* (*left*) shows representative traces of whole-cell barium currents (I_{Ba}) flowing through HVACCs in cultured postnatal DRG neurons (5-to 11-d-old), evoked at several membrane potentials from a holding potential (V_H) of −70 mV. The currents had an activation threshold and peak of approximately −30 and 0 mV, respectively (Fig. 1*A*, *right*). The absence of an early inactivating component (Fig. 1*A*, *left*) and the lack of an extra current peak ("shoulder") at relative negative potentials in the current–voltage (*I–V*) curve (Fig. 1*A*, *right*) indicated a negligible low-threshold T-type current contribution at this V_H, as reported in these cells by others (Scroggs and Fox, 1991).

Bath application of 1 μM DADLE, a DOR-preferring enkephalin analog (Bot et al., 1997, and references therein) that mimics the action of natural enkephalins on synaptic transmission (Mulder et al., 1984), reversibly inhibited I_{Ba} in 37% of 457 cells tested 3–96 hr after plating. Figures 1*B* and 3, *A* and *C*, show actual records and the time course of the response. On average, 1 μM DADLE inhibited 31.6 ± 16.3% (n = 168) of I_{Ba}, as estimated from the current reduction at the end of the depolarizing test pulse.

I–V curves of I_{Ba} obtained before and during DADLE application illustrate the agonist effect at the end of 25 msec voltage test pulses over a wide membrane potential range (Fig. 1*B*, *right*). The inhibition was most conspicuous at the peak of the curve (0 mV), which did not apparently shift along the voltage axis, and became less obvious at depolarized potentials as a result of its voltage dependence. Whereas these data reflect the sum of effects of the agonist on the individual *I–V* curves of the potentially targeted HVACC components, it has been shown that neurotransmitters affect such curves in a similar way (Patil et al., 1996; Roche and Treistman, 1998). We tested the agonist effect at 0 mV at the end of 20–50 msec test pulses to clearly resolve the reduction in current magnitude induced by δ agonists. These measurements, however, overlook the maximal effect of the agonist, which occurs very early after the onset of the test pulse (Fig. 1*B*, *trace D*), and subtle differential effects of the agonist on the voltage dependence of individual current components.

The inhibited current exhibited a slow activation phase (Fig. 1*B*, *trace D*) that reflected the commonly observed voltage- and time-dependent removal of neurotransmitter-induced G-protein-mediated inhibition of non-L-type HVACC currents (Hescheler et al., 1987; Bean, 1989; Carbone and Swandulla, 1989; López and Brown, 1991; Kasai, 1992; Rusin and Moises, 1995; Albillos et al., 1996; Wiley et al., 1997). The voltage dependence of the DADLE-induced inhibition was further confirmed by showing that a depolarizing prepulse to 40 mV, preceding the test pulse, partially removed the inhibition observed at 0 mV (Fig. 1*C*). On

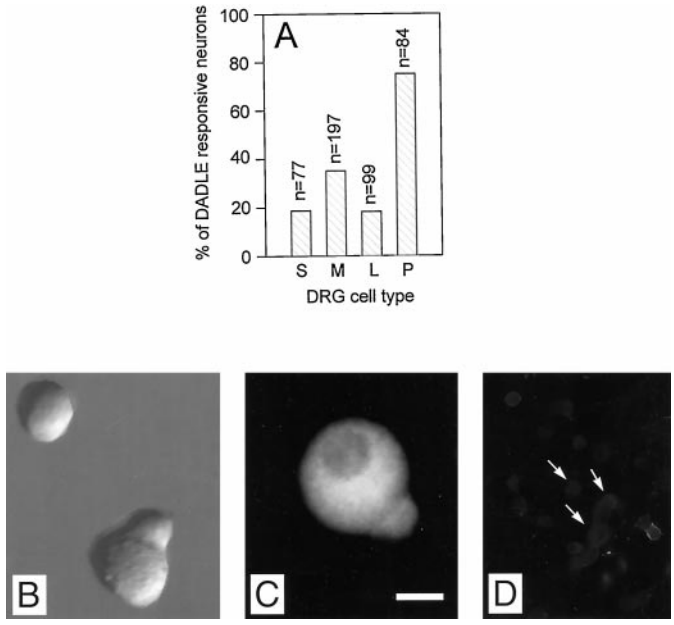

Figure 2. Percentage of DADLE-responding cells in different neuron subpopulations. *A,* The percentages of DADLE-responsive neurons in the subpopulations of small (*S*), medium (*M*), and large (*L*) neurons and medium-sized P-neurons (*P,* from pear-shaped) were 18.7, 35, 18.2, and 75%, respectively. The number of cells tested appear on *top* of the *bars*. The relative fractional contribution of each cell type to the total population in culture was 58 (*S*), 26 (*M*), 9 (*L*), and 7% (*P*). *B,* P-neuron under Nomarski phase contrast cultured for 20 hr. A small round neuron is also visible in the field. *C*, *D*, An antibody against substance P labeled all P-neurons (an example is shown in *C*), but only a fraction of the other cells types (*arrows* in *D* show examples of nonlabeled cells). Cells after 24 hr in culture. Scale bar: *B*, *C*, 10 μm; *D*, 40 μm.

average, the prepulse recovered 39.3 ± 6.2% ($n = 10$) of the DADLE-sensitive current (I_D).

The frequency of responding cells varied among the subpopulations recognized *in vitro* but not with postnatal age (P5–P11) or animal sex. Grouped according to the diameter of their round-shaped soma (Gilabert and McNaughton, 1997), small (<15 μm), medium (15–26 μm), and large (>26 μm) neurons contributed 58, 26, and 9%, respectively, to the total population *in vitro.* DADLE inhibited I_{Ba} in 19 ($n = 77$), 35 ($n = 197$), and 18% ($n = 84$) of the cells in those groups, respectively (Fig. 2*A*). In addition, we identified a novel subpopulation of medium-sized neurons featuring an unmistakable "pear-shaped" cell body of ~15 × 26 μm, which we will refer to as P-neurons after their distinctive morphology. They represented the 7% of the population in culture and were found at all postnatal ages examined (P5–P11) in similar proportions in cephalic, middle, and caudal DRGs. In sharp contrast to the other cell types, DADLE inhibited I_{Ba} in 75% ($n = 84$) of the P-neurons (Fig. 2*A*).

The unusual morphology of P-neurons did not appear to result from the dissociation process, culture conditions, or cell injury. First, their shape was maintained in long-term cultures (up to 12 d). Second, they exhibited functional and morphological properties of healthy neurons, such as the expression of several types of voltage-dependent ion currents (Na^+, K^+, and Ca^{2+}), and the development of axons when maintained in culture for several days. Third, they were present in cultures growing on three different substrates (poly-D-lysine plus collagen, poly-D-lysine, or laminin), maintained in either defined media or media supplemented with serum. Interestingly, every single P-neuron in culture showed intense somatic immunoreactivity for the pain-related peptide substance P (Fig. 2*C*).

The enkephalin analog DADLE has a remarkable high affinity for DORs and interacts with both known pharmacological DOR subtypes (Xu et al., 1998). A series of experiments showed that DORs mediated the DADLE-induced HVACC current inhibition. First, naltrindole (1 μM), a highly selective DOR antagonist (Rogers et al., 1990; Reisine, 1995), powerfully blocked the effect of DADLE (Fig. 3*A*) in cells previously shown to be sensitive to the enkephalin agonist. The current traces of Figure 3*A* (*right*) show one of several tests ($n = 5$) in which 1 μM naltrindole completely prevented the DADLE-induced inhibition. Never did DADLE inhibit more than 5% of I_{Ba} in the presence of naltrindole, which by itself had no effect on I_{Ba}. The lack of DADLE effect in the presence of naltrindole was not caused by receptor desensitization (McFadzean and Docherty, 1989; Motin et al., 1995). To avoid desensitization of the DOR-mediated response, the DOR agonist was applied, at most, twice and just long enough to achieve a maximal effect (1.5–2 min). Desensitization was negligible with such procedure as revealed by the essentially similar inhibitions during two consecutive control DADLE applications (Fig. 3*B*). Naloxone (2 μM), a nonselective opioid receptor antagonist, also blocked the DADLE-induced I_{Ba} inhibition (data not shown). Second, in DADLE-responsive cells, the DOR-2-selective agonist deltorphin-II (100 nM), but not the DOR-1-selective agonist DPDPE (1 μM), mimicked the DADLE-induced HVACC current inhibition ($n = 5$), independently of the order of application (Fig. 3*C*). The smaller inhibition observed with deltorphin-II could have resulted from the use of a 10-fold smaller concentration (100 nM) or differences in the mode of action of the agonists. At such a concentration, on the other hand, only DORs-2 were probably activated. For example, deltorphin-II is 900 times more selective for DORs-2 than μ opioid agonists (Buzas et al., 1992), also known to inhibit Ca^{2+} currents in sensory neurons (Rusin and Moises, 1995). Conversely, for achieving 50% of the effect of 1 μM [D-Ala^2-*N*-Me-Phe^4-$Glycol^5$]-enkephalin (DAMGO) (a μ opioid receptor agonist) on synaptic currents in spinal cord, a 100-fold larger concentration of deltorphin-II was required (Glaum et al., 1994). The deltorphin-II-induced HVACC current inhibition and the lack of DPDPE effect were confirmed in several other cells in which those agonists were tested individually ($n = 5$ and 6, respectively). Third, whenever DADLE was ineffective, neither deltorphin-II nor DPDPE were effective in experiments in which either all three agonists ($n = 8$) or DADLE and DPDPE ($n = 5$) were tested sequentially in the same cell. This excluded the possibility that the DOR-2-selective agonist inhibited I_{Ba} via receptors not activated by DADLE. The lack of DPDPE effect was consistent with previous reports (Schroeder et al., 1991). The involvement of DORs-2, on the other hand, may explain why DOR-mediated HVACC modulation passed previously unnoticed.

Because DADLE could potentially interact with MORs (Goldstein and Naidu, 1989), we ran experiments to assess the involvement of that receptor in the DADLE response. The irreversible MOR antagonist β-funaltrexamine (β-FNA) (5–10 μM) (Takemori et al., 1981) had no effect on the DADLE response ($n = 5$) (Fig. 4*A*). The slightly smaller inhibition during the second DADLE application (Fig. 4*A*) was attributable to DADLE acting on an initially smaller agonist-sensitive current because of a matching deficit in current recovery after the first agonist expo-

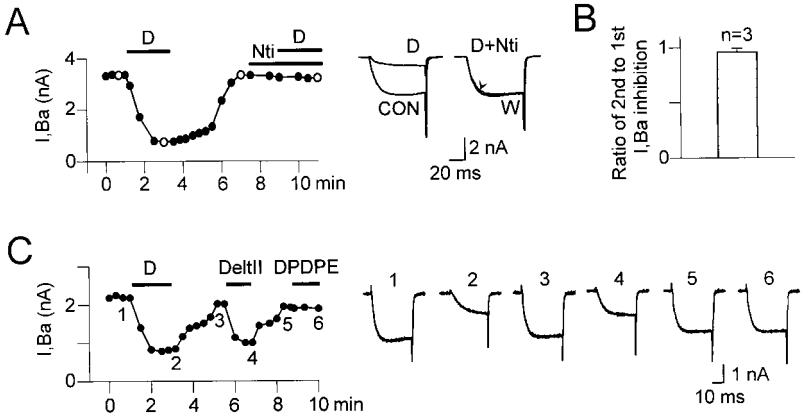

Figure 3. DOR involvement in the DADLE-induced inhibition of I_{Ba}. *A*, Plot of time course (*left*) and I_{Ba} current records (*right*) corresponding to *open symbols* of an experiment testing the effect of the highly selective DOR antagonist naltrindole (*Nti*) on the DADLE-induced inhibition. I_{Ba} was elicited with 60 msec pulses to 0 mV from a V_H of −70 mV. The data points in the plot correspond to I_{Ba} values at the end of the test pulses. The control current (*trace CON*) was powerfully inhibited by 1 μM DADLE (*trace D*), and the inhibition fully reversed upon agonist washout (*trace W*). DADLE was completely ineffective when subsequently co-applied with 1 μM naltrindole (*trace D+Nti*). The lack of DADLE effect in the presence of naltrindole was not attributable to response desensitization (*B*). *B*, The responses to short (1.5–2 min) applications of DADLE, as used in our experiments, were not affected by desensitization. Two applications of DADLE of 2 min each, separated by an interval of 3–5 min, caused a similar amount of I_{Ba} inhibition in control cells ($n = 3$), as illustrated by the plot of the ratio of the magnitudes of the second to the first I_{Ba} inhibition (essentially 1). Ratios in the individual cells were 0.93, 0.95, and 0.99. *C*, Time course (*left*) and current records (*right*) of an experiment in which the DOR-2-selective agonist deltorphin-II (100 nM) mimicked the DADLE-induced inhibition (*traces 1–3*) of I_{Ba} in a reversible way (*trace 3–5*). Current records correspond to similarly numbered data points in the time course plot. As in other four cells, 1 μM DPDPE (a DOR-1-selective agonist) had no effect on I_{Ba} (*trace 6*). In this cell, DADLE and deltorphin-II (*Delt-II*) reduced 1.4 and 1.02 nA of I_{Ba}, respectively.

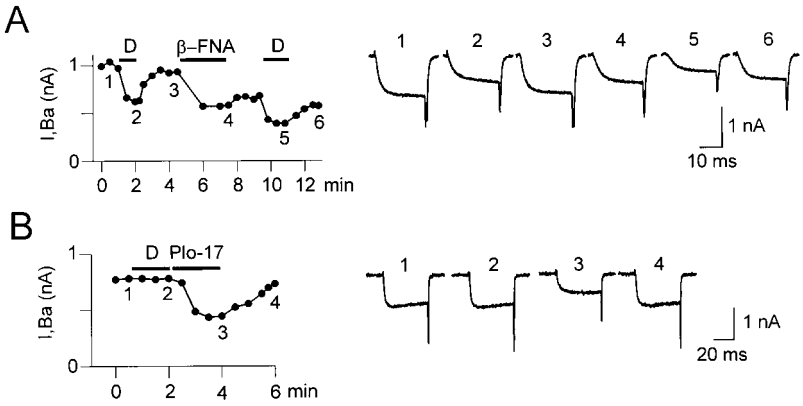

Figure 4. The DADLE response does not involve MOR. *A,* Time course (*left*) and corresponding traces (*right*) showing the reversible response to DADLE before (*traces 1–3*) and after (*traces 4–6*) the irreversible block of MOR with 5 μM β-FNA, a MOR-selective antagonist. In this and in other four cells, β-FNA had no effect on the reversible DADLE-induced inhibition. The reduction of I_{Ba} during β-FNA application results from the κ opioid activity of this compound. *B,* The MOR-selective agonist PLO-17 (1 μM) reversibly inhibited I_{Ba} (*traces 2–4*) in a cell in which DADLE (1 μM) was ineffective (*traces 1*, *2*). Records from a P-neuron. Similar results were found in six cells. The MOR-mediated I_{Ba} inhibition did not show desensitization. In all experiments, V_H was −70 mV, and the test voltage pulses were 0 mV. Current records in *A* and *B* correspond to similarly numbered data points in their respective time course plots.

sure or because of a possible modest DOR block by β-FNA (Hayes et al., 1985). As a result, I_D decreased to 89.5 ± 5.4% of control ($n = 5$) during the second DADLE application. As noted by Schroeder et al. (1991), the current inhibition observed during β-FNA application results from a κ opioid agonist activity of β-FNA (Takemori et al., 1981) and served as a positive control for the effectiveness of that drug. The highly selective MOR agonist PLO17 could reversibly inhibit the HVACC current in cells in which DADLE was ineffective ($n = 6$) (Fig. 4*B*). This showed that PLO17, but not DADLE, activated MORs, a finding replicated in several other neurons. Similarly, DAMGO, but not DADLE or DPDPE, inhibited K^+ currents in hippocampal neurons (Moore et al., 1994). Lastly, both DADLE and deltorphin-II responses desensitized if those agonists were present in the bathing solution for over 1 min once the inhibition of HVACC currents reached a stable level (data not shown). In contrast, the MOR-mediated HVACC current inhibition does not desensitize (Schroeder et al., 1991). Finally, the overall low frequency of cells responding to DADLE (37%) was much smaller than that of sensory neurons responding to MOR activation (90%) (Schroeder et al., 1991; Rusin and Moises, 1995). Together, our data strongly indicate that DORs, but not MORs, mediate the DADLE-induced HVACC current inhibition and suggest that DORs-2 are probably involved.

It is unlikely that kappa opioid receptors (KORs) mediated the DADLE effect because the irreversible κ-mediated inhibition caused by β-FNA did not occlude or reduce the DADLE response (Fig. 4*A*), and the affinity of DADLE for KORs is four orders of magnitude smaller than that for DORs (Goldstein and Naidu, 1989).

HVACC currents in postnatal sensory neurons

The contributions of L-, N-, P-, and Q-type HVACC currents to I_{Ba} were estimated as the current fractions blocked by 10 μM nimodipine, 2 μM ω-CTx-GVIA, 50 nM ω-Aga-IVA, and 0.5–1 μM ω-CTx-MVIIC, respectively (Llinás et al., 1989; Regan et al., 1991; Randall and Tsien, 1995; McDonough et al., 1996). Figure 5*A* summarizes the data. A current fraction (5.6 ± 2.2%; $n = 5$) remained unblocked in the presence of all drugs together and will be referred to as R-type (Randall and Tsien, 1995). Cd^{2+} (300 μM) completely blocked it, indicating that it was carried by voltage-activated Ca^{2+} channels (data not shown). Consistent with reports showing that postnatal sensory neurons *in vitro* express all HVACC current types (Scroggs and Fox, 1991; Moises et al., 1994; Rusin and Moises, 1995), any given Ca^{2+} channel blocker always inhibited a fraction of the total whole-cell I_{Ba} in every single neuron tested.

The average L-type (18.2 ± 4.5%; $n = 10$) and N-type (48.5 ± 11.5%; $n = 8$) contributions to I_{Ba} agreed very well with published data in these cells [$L = 15\%$; N = 42% (Rusin and Moises, 1995); and $L = 18\%$; N = 43% (Mintz et al., 1992)]. The effect of ω-CTx-GVIA was essentially irreversible (Fig. 5*B*), ruling out a potential block of L-type currents by that drug reported to be reversible and to require a much larger concentration (Williams

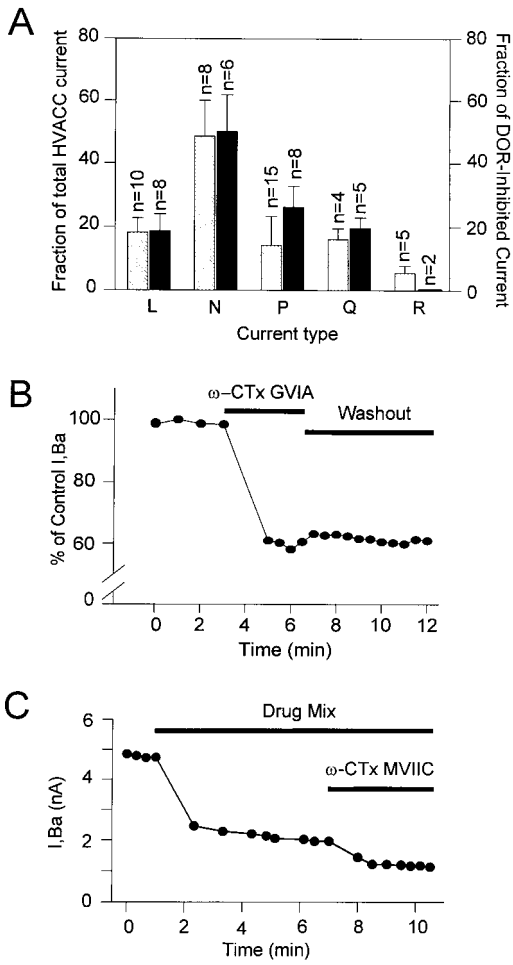

Figure 5. HVACC currents inhibited by toxins and targeted by DORs. *A, Striped bars* show the average ± SEM contributions of L-, N-, P-, and Q-type HVACC currents to the whole-cell I_{Ba}. These values were taken as equal to the percentages of I_{Ba} inhibited by 10 μM nimodipine (*L*), 2 μM ω-CTx-GVIA (*N*), 50 nM ω-Aga-IVA (*P*), and 0.5–1 μM ω-CTx-MVIIC (*Q*), respectively. Because of its lack of selectivity, ω-CTx-MVIIC was applied after N-, P-, and L-type currents were all previously blocked. The R-type was defined as the fraction that remained unblocked in the presence of all above drugs (*R*) and was fully blocked by Cd^{2+}. *Solid bars* show the average ± SEM contributions of each current type to the DADLE-sensitive current (I_D). Notice the large contribution of the P-type current to I_D despite its relatively small contribution to I_{Ba}. *B,* Plot of I_{Ba} versus time before and after the application of 2 μM ω-CTx-GVIA. The data points represent values of I_{Ba} at the end of 40 msec depolarizing test pulses to 0 mV from a V_H of −70 mV. The ω-CTx-GVIA-induced inhibition stabilized within 2 min and was essentially irreversible (tested up to 20 min). In this neuron, the N-type current contributed 40% of I_{Ba}. To better visualize the toxin effect, the ordinate axis was truncated. Data from a medium-sized, round neuron. *C,* Time course from an experiment testing the contribution of the Q-type current to I_{Ba}, which was evoked with 20 msec test pulses. The L, N, and P currents contributing to the initial I_{Ba} were blocked by a combination (*Drug Mix*) of 10 μM nimodipine, 2 μM ω-CTx-GVIA, and 50 nM ω-Aga-IVA. The fraction subsequently inhibited by 0.5 or 1 μM ω-CTx-MVIIC (1 μM in this cell) was defined as Q-type. The time course graph plots the values of I_{Ba} at the end of the test pulses. The current remaining unblocked was defined as R-type. Data from a P-neuron. All measures made at the end of voltage test pulses to 0 mV from a V_H of −70 mV.

et al., 1992). We defined the P-type fraction as that blocked with 50 nM ω-Aga-IVA, a concentration that maximally inhibits P-type Ca^{2+} channels in cerebellar and peripheral sensory neurons (Mintz and Bean, 1993; Tottene et al., 1996) and spares other HVACC currents (Mintz et al., 1992; Rusin and Moises, 1995). The average P-type contribution was 14.2 ± 9.1% (n = 15). Others estimated a larger P-type contribution with 200 nM ω-Aga-IVA (23% in Mintz et al., 1992; 24% in Rusin and Moises, 1995), a result that we replicated with that concentration (25.2 ± 8.4%; n = 6). However, we used 50 nM ω-Aga-IVA to define the P-type contribution because higher concentrations could also affect Q-type channels (IC_{50} of ~90 nM) (Randall and Tsien, 1995). ω-Aga-IVA did not affect N- or L-type currents. Thus, the average current inhibition obtained with 50 nM ω-Aga-IVA plus 2 μM ω-CTx-GVIA together (61%; n = 3; 53, 62, and 68% in each individual cell) was similar to the sum (62%) of the inhibitions obtained separately with each toxin (14% with 50 nM ω-Aga-IVA; 48% with 2 μM ω-CTx-GVIA), indicating that those drugs, at those concentrations, inhibited separate Ca^{2+} channel populations. Accordingly, a much higher ω-Aga-IVA concentration did not affect the L current in central and peripheral sensory neurons (Mintz et al., 1992).

The pharmacological identification of the Q-type current relied on its blockade by ω-CTx-MVIIC, a drug that can also block ω-CTx-GVIA-sensitive N-type channels and ω-Aga-IVA-sensitive P-type channels in rat neurons (Randall and Tsien, 1995; McDonough et al., 1996). Therefore, we followed the standard procedure of measuring the effect of ω-CTx-MVIIC on the current remaining after blocking the non-Q- and non-R-type currents with 10 μM nimodipine, 2 μM ω-CTx-GVIA, and 50 nM ω-Aga-IVA (Fig. 5*C*) (Randall and Tsien, 1995; Rusin and Moises, 1995; McDonough et al., 1996). The time needed for the drug mixture to reach a stable effect varied among cells (3–7 min), reflecting the relatively slow speed of bath solution exchange and cell-to-cell variability. Subsequently, ω-CTx-MVIIC caused a partial and irreversible inhibition (Hillyard et al., 1992; Rusin and Moises, 1995). The average Q fraction estimated with 0.5–1 μM ω-CTx-MVIIC was 16.1 ± 3.4% (n = 4), somewhat larger than that of DRG neurons from older rats (P14–P28; 10%) (Rusin and Moises, 1995) and smaller than that of rat cerebellar neurons (35%) (Randall and Tsien, 1995). As in other work (Randall and Tsien, 1995), 0.5 μM ω-CTx-MVIIC caused a saturating effect, although the inhibition reached a plateau sooner with 1 μM (1.5 vs 3 min).

HVACC current types inhibited by DORs

A second series of experiments determined which HVACC current types were inhibited by DADLE and their fractional contribution to I_D. The data are from neurons in which the HVACC current showed negligible rundown over the entire experiment, and the DADLE-induced inhibition was fully reversible. We found that the DOR-mediated I_{Ba} inhibition targeted all HVACC current types. The average contributions of the L-, N-, P-, and Q-type HVACC currents to I_D were 18.7 ± 5.3% (n = 8), 50.1 ± 11.7% (n = 6), 26.2 ± 6.5% (n = 8), and 19.6 ± 3.3% (n = 5), respectively. These values correspond to DADLE inhibiting 32.5, 32.6, 58.3, and 38.5% of L-, N-, P-, and Q-type currents, respectively. No differences were apparent between the various sensory subpopulations. The total sum of percentages in excess of 100% may reflect either the different expression levels of HVACC current types in neurons of different sizes (Scroggs and Fox, 1991) or less than perfect toxin selectivity. Figure 5*A* compares the average contributions of each current type to I_{Ba} and I_D. No matter how large a reduction of I_D a particular Ca^{2+} channel blocker caused, no single blocker ever fully occluded the

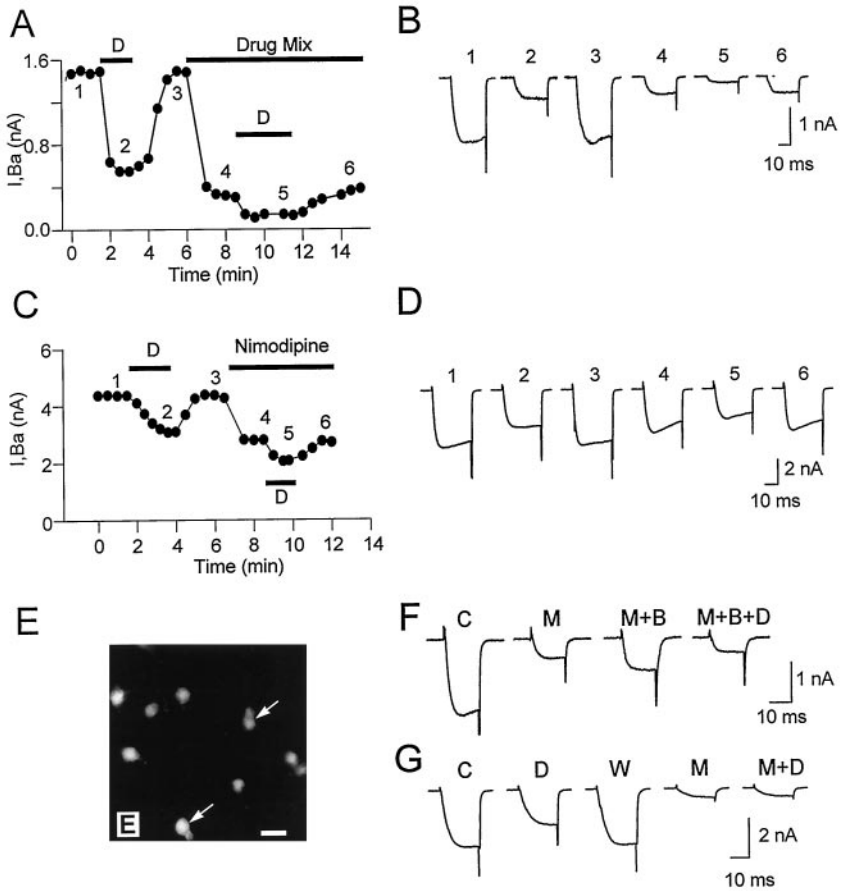

Figure 6. DOR-mediated inhibition of the dihydropyridine-sensitive L-type current. Data points in *A* and *C* represent values of I_{Ba} at the end of 25 msec test pulses to 0 mV from a V_H of −70 mV. *A,* Time course of an experiment testing the L-type current contribution to I_D with protocol-1. The first DADLE application reversibly inhibited 63% of I_{Ba}. Subsequently, the block of N-, P-, and Q-type currents with 2 μM ω-CTx-GVIA, 50 nM ω-Aga-IVA, and 1 μM ω-CTx-MVIIC (*Drug Mix*) inhibited 81% of I_{Ba}. The contribution of the L-type current to I_D was revealed by a second DADLE application, which inhibited 53% of the non-N, non-P, and non-Q currents in a fully reversible way. *B,* Current records corresponding to similarly numbered data points in *A*. *C,* Time course of an experiment testing the L-type contribution to I_D with protocol-2. The block of the L-type current fraction (36% in this cell) with 10 μM nimodipine reduced the amount of I_{Ba} inhibited by 1 μM DADLE. The second DADLE application was done in the continuous presence of nimodipine. *D,* Current records corresponding to similarly numbered data points in *C*. The current reversibly inhibited by DADLE decreased from 1.3 to 0.74 nA after blocking the L-type current with 10 μM nimodipine. *E*, All sensory neurons in culture, regardless of cell subpopulation, were immunoreactive for the α_{1C} subunit of neuronal Ca^{2+} channels, indicating the presence of L-type HVACC in these cells. Neurons obtained from 5-d-old postnatal animals. P-neurons in the culture are labeled with *arrows*. Scale bar, 20 μm. *F*, The control HVACC current (*trace C*), activated by voltage pulses to 0 mV from a V_H of −70 mV, was partially blocked by a mixture of 2 μM ω-CTx-GVIA, 50 nM ω-Aga-IVA, and 1 μM ω-CTx-MVIIC, which was kept in the bath for the rest of the experiment (*trace M*). *S*-(±)-Bay-K 8644 (10 μM) increased the amplitude of the drug mixture-resistant current (*trace M+B*), and the subsequent application of 1 μM DADLE in the continuous presence of Bay-K 8644 reduced the enhanced current (*M+B+D*). The magnitude of the inward current in the presence of DADLE was smaller than that before *S*-(±)-Bay-K 8644 application. *G,* The R-type current, defined as the current remaining unblocked in the presence of a mixture of 10 μM nimodipine, 2 μM ω-CTx-GVIA, 50 nM ω-Aga-IVA, and 1 μM ω-CTx-MVIIC (*trace M*), was completely insensitive to DADLE (*trace M+D*). The agonist reversibly inhibited I_{Ba} before the application of the drug mixture (*traces C, D, W*). Data from a P-neuron.

DADLE-induced inhibition. Analogously, no matter how small the magnitude of the δ opioid inhibition was, any given HVACC current type tested (except the R-type) was always found to contribute to I_D. Representative data for each HVACC current type will be reported separately below.

L-type current

Both protocol-1 ($n = 3$) and protocol-2 ($n = 5$) indicated that the L-type HVACC current contributed to I_D. Figure 6*A* shows time course data (*left*) and actual current records (*right*) from a representative cell tested with protocol-1. A first application of 1 μM DADLE inhibited 0.95 nA (63%) of the control I_{Ba} in a fully reversible way (Fig. 6*A*,*B*, *traces 1–3*). The combined application of 2 μM ω-CTx-GVIA, 50 nM ω-Aga-IVA, and 1 μM ω-CTx-MVIIC inhibited the non-L- and non-R-type currents (1.18 nA; 81%) (Fig. 6*A*,*B*, *traces 3*, *4*). A second application of DADLE reversibly inhibited 0.16 nA of the remaining current, presumably consisting only of L- and R-type components (Fig. 6*A*,*B*, *traces 4–6*). Because the R-type current was agonist-insensitive (Fig. 6*G*) ($n = 2$), we concluded that DADLE inhibited the L-type component. The magnitudes in the reduction of I_D after blocking the L-type or other current types in the experiments reported below (at least 19%) are incompatible with desensitization (at most 7%) (Fig. 3*B*). Electrophysiological and immunocytochemical data support our assumption that the current fraction remaining in the presence of 2 μM ω-CTx-GVIA, 50 nM ω-Aga-IVA, and 1 μM ω-CTx-MVIIC contained an L-type component. All types of sensory neurons in culture always express a nimodipine-sensitive L-type component (Kostyuk et al., 1988; Cardenas et al., 1995; Rusin and Moises, 1995). Consistently, we found that a highly specific antibody against rat and mouse α_{1C} subunits of neuronal L-type HVACC (Hell et al., 1993) strongly labeled the soma of every single sensory neuron in culture, in ~500 cells examined (Fig. 6*E*).

The contribution of L-type current to I_D was further validated by using protocol-2. In this case, a first application of DADLE reversibly inhibited 1.3 nA of I_{Ba} (29%) (Fig. 6*C*,*D*). After reversal of the agonist effect, application of the L-type channel blocker nimodipine (10 μM) inhibited 36% of I_{Ba} (1.59 nA). A second application of DADLE, in the continuous presence of nimodipine, only inhibited 0.74 nA. Because the suppression of the nimodipine-sensitive fraction reduced the amount of current inhibited by DADLE, we again concluded that I_D had an L HVACC current component. Lastly, the L-type current agonist Bay-K 8644 (10 μM) (Fox et al., 1987) increased the current remaining in the presence of ω-CTx-GVIA, ω-Aga-IVA, and ω-CTx-MVIIC, indicating the presence of an L-type component in the drug mixture-insensitive fraction (Fig. 6*F*). DADLE reduced the enhanced current to an amplitude smaller than that before Bay-K 8644 application (Fig. 6*F*, *trace M+B+D*). Together, our results strongly support that the L-type current con-

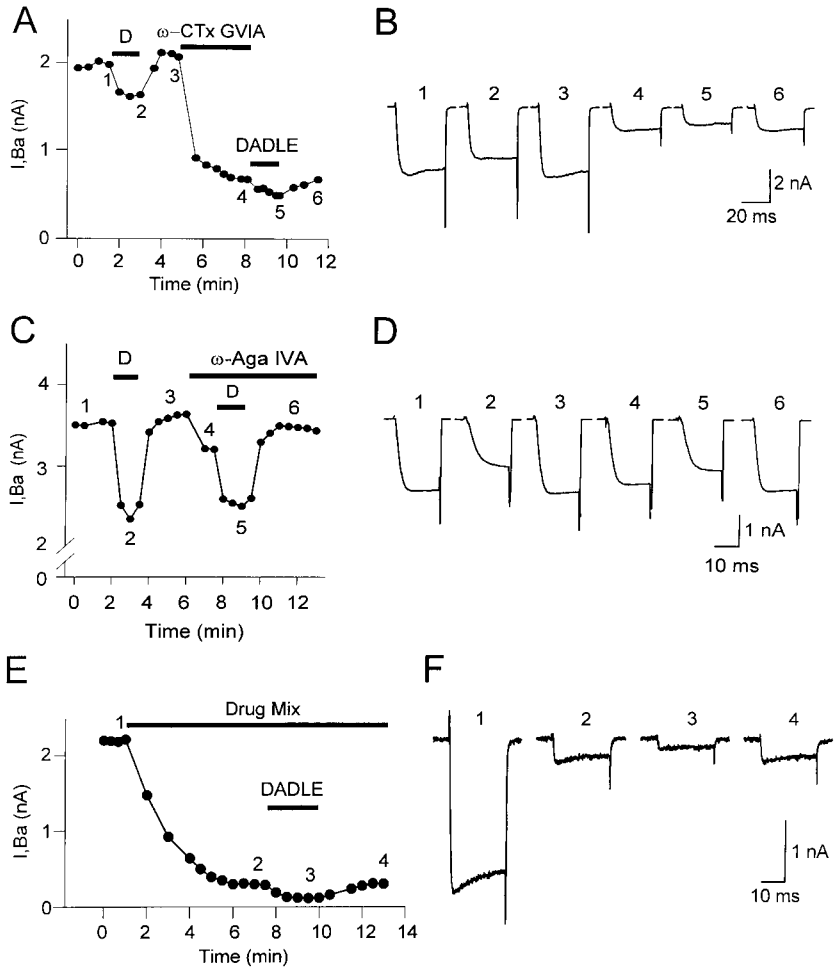

Figure 7. DOR-mediated inhibition of N-, P-, and Q-type currents. *A*, Time course of an experiment testing the N-type current contribution to I_D. The block of the N-type current fraction by 2 μM ω-CTx-GVIA reduced the amount of I_{Ba} inhibited by 1 μM DADLE. *B*, Current records corresponding to similarly numbered data point of the experiment in *A*. DADLE reversibly inhibited 0.35 nA of the initial I_{Ba} (*traces 1–3*). After the application of 2 μM ω-CTx-GVIA, which inhibited 1.4 nA of I_{Ba} (*trace 4*), a second DADLE application reversibly inhibited 0.18 nA of the remaining non-N current (*traces 4–6*). *C*, Time course of an experiment testing the P-type current contribution to I_D. The data points represent values of I_{Ba} at the end of 25 msec voltage test pulses to 0 mV from a V_H of −70 mV. The block of the P-type current fraction (11.8% in this cell) with 50 nM ω-Aga-IVA reduced the amount of I_{Ba} inhibited by 1 μM DADLE. The toxin was present throughout the second DADLE application because its effect was partially reversible. *D*, Current records corresponding to similarly numbered data points in *C*. The first DADLE application reversibly inhibited 1.2 nA of the total I_{Ba} (*traces 1–3*), whereas the second agonist application, after the block of the P-type current, suppressed only 0.72 nA of the non-P I_{Ba} (*traces 4–6*). Because the magnitude of the inhibited I_{Ba} was larger during the second (*trace 5*) than during the first DADLE application (*trace 2*), the effect of DADLE deceptively appeared to be smaller than predicted from the loss of target, ω-Aga-IVA-sensitive P-type channels. This occurred because the second DADLE application was tested on the larger preagonist current (*trace 3* vs *trace 1*) resulting from the over-recovery of I_{Ba} during reversal of the first DADLE-induced inhibition (*trace 3*; see data points in *C*). When allowances are made for this change in the basal I_{Ba}, the reduction in DADLE-induced inhibition can be entirely accounted for by the suppression of P-type target channels. *E*, *F*, Time course and corresponding traces from a representative experiment in a round neuron, using protocol-1 to test the contribution of Q-type HVACC current to I_D. The *numbered points* in *E* correspond to similarly *numbered traces* in *F*. N-, P-, and L-type HVACC currents were inhibited by perfusing the cell with a solution containing 2 μM ω-CTx-GVIA, 50 nM ω-Aga-IVA, and 10 μM nimodipine (*Drug Mix*; *traces 1, 2* in *F*). DADLE reversibly inhibited a fraction of the remaining non-N, non-L, and non-P currents (*traces 2, 3* in *F*). This inhibition was fully reversible (*trace 4* in *F*). The data points are the values of I_{Ba} at the end of 20 msec voltage test pulses to 0 mV from a V_H of −70 mV.

tributes to I_D. The average contribution, estimated from data obtained with protocols-1 and -2, was 18.7 ± 5.3% (n = 8).

N-type current

Figure 7, *A* and *B*, shows representative data on the contribution of N-type channels to I_D obtained with protocol-2. In this example, the first DADLE application reversibly reduced I_{Ba} by 0.35 nA (*traces 1–3*), amounting to an inhibition of 13% of the control current. *Trace 4* shows the current that remains after the selective inhibition of the N-type fraction with 2 μM ω-CTx-GVIA. The irreversible ω-CTx-GVIA-induced block reached a plateau within 2 min. In the neuron of Figure 7, the ω-CTx-GVIA-sensitive N-type current amounted to 1.4 nA and therefore contributed 67% of the total I_{Ba}. Blockade of this fraction caused a reduction of the I_{Ba} inhibition by a second DADLE application, which reduced the non-N-type current by 0.18 nA in a fully reversible manner (*traces 5*, *6*). The N-type current contribution to I_D ranged from 31 to 69% in different cells, with an average of 50.1 ± 11.7% (n = 6). The average does not include one cell in which the contribution of N-type current to I_D was particularly large (84%). That case shows, however, that no matter how large a contribution a given current type made to I_D, it never accounted for the totality of it.

P-type current

The P-type current contributed to I_D in all tested neurons (n = 8). Representative data, obtained with protocol-2 in a P-neuron, are illustrated in Figure 7, *C* and *D*. In the absence of the toxin, DADLE reversibly reduced I_{Ba} by 1.2 nA, which represented a 34% inhibition of the control current (Fig. 7*C*, *traces 1–3*, *D*). After recovery of I_{Ba} upon agonist washout, bath application of 50 nM ω-Aga-IVA inhibited 0.43 nA (11.8%) of the current when measured at the end of the 25 msec voltage test pulse (Fig. 7*C*,*D*, *trace 4*). A second application of DADLE, done in the presence of the toxin to ensure no recovery of P-type current, reduced I_{Ba} by only 0.72 nA (Fig. 7*C*,*D*, *trace 5*). In this cell, the ω-Aga-IVA-sensitive current contributed 35.8% of I_D. Similar results were observed in all tested cells, indicating that P-type HVACC are targeted by DORs. The average P-type contribution to I_D was 26.2 ± 6.5% (n = 8), ranging from 13.4 to 35.8% in different cells. Interestingly, in the cell of Figure 7, *C* and *D*, as well as in five of eight other cells tested, DADLE appeared to inhibit the entire P-type fraction, because the absolute reduction in I_{Ba} inhibition after the block of the P-type current (0.48 nA) (Fig. 7*D*, *trace 5*) almost exactly agreed with the amount of current inhibited by the toxin (0.43 nA) (Fig. 7*D*, *trace 4*). However, this finding should be

interpreted cautiously because the small contribution of the P-type current to the total HVACC current could lead to uncertainties in these measurements.

Q-type current

Data gathered with protocol-1, which assessed the effect of a single application of DADLE after the non-Q- and non-R-type currents were previously inhibited with 10 μM nimodipine, 2 μM ω-CTx-GVIA, and 50 nM ω-Aga-IVA, indicated that the Q current contributed to I_D. Figure 7 shows representative time course data (*E*) and current records (*F*). The blocker mixture (*Drug Mix*) inhibited ~86% of the total I_{Ba} of this cell. A subsequent application of 1 μM DADLE, in the continuous presence of the blockers, reversibly inhibited 0.18 nA (61%) of the remaining current (Fig. 7*E*,*F*, *traces 2–4*), which includes a DADLE-insensitive R fraction. These data indicated that Q-type HVACC were also a target of the DOR-mediated inhibition and were replicated in four other cells. In the example of Figure 7, *E* and *F*, the contribution of the Q- plus -R type currents to I_{Ba} was 14% (from the current remaining after applying the drug mixture), and the amount of Q-type current inhibited by DADLE represented 8% of the initial I_{Ba}. On average, these quantities, in five cells, were 22 ± 11 and 6 ± 2%, respectively. Subtracting the previously estimated R fraction (5.6%) to the R plus Q fraction (22%) yields a Q fraction (16.4%) that closely agrees with that directly estimated (16.1%). Because in this series of experiments DADLE was applied only once, the average contribution of the Q-type current to I_D (19.6 ± 3.3%; $n = 5$) was estimated with respect to the average magnitude of I_D, previously measured in 168 cells.

DISCUSSION

DOR-mediated HVACC current inhibition

This work represents the first demonstration that DORs inhibit HVACC currents in sensory neurons. It validates a cellular mechanism long suspected to mediate the inhibitory effects of δ opioids on synaptic transmission and pain sensation in sensory circuits (Jessell and Iversen, 1977; Dickenson et al., 1987; Collin et al., 1991; Glaum et al., 1994; Zachariou and Goldstein, 1996). Our finding that DORs target several types of HVACC currents further suggests that they could broadly affect HVACC-mediated Ca^{2+} signaling in neurons.

Substantial evidence supports the existence of two pharmacological subtypes of DORs, termed DORs-1 and DORs-2 (Sofuouglu et al., 1991; Mattia et al., 1992; Bilsky et al., 1996; Reisine, 1995). The DADLE-induced inhibition of the HVACC current implicates DORs because the highly selective DOR antagonist naltrindole (Stewart and Hammond, 1994) fully blocks it. Deltorphin-II, a natural compound exquisitely selective for DORs-2 (Erspamer et al., 1989), mimics the DADLE effect, whereas a DOR-1 agonist has no effect. These results indicate a primary role of DORs-2 in the inhibitory effect of DADLE. Like the endogenous enkephalins, DADLE has a very high affinity for either native DOR subtypes, as well as the cloned DOR (categorized as DORs-2) (Kieffer et al., 1992; Raynor et al., 1994; Wang et al., 1996; Xu et al., 1998). The ability of DADLE to inhibit Ca^{2+} currents entirely via DORs is patently shown in NG108–15 cells, which express only those opioid receptors (Tsunoo et al., 1986; Hescheler et al., 1987; McFadzean and Docherty, 1989). In nonsensory neurons, DADLE and Leu-enkephalin produce similar inhibitory effects via DOR on Ca^{2+} and K^+ currents (Moore et al., 1994; Motin et al., 1995). Because it was observed only in DADLE-responsive cells, the deltorphin-II effect necessarily involves receptors that sustained the DADLE response. Recent reports implicating DORs-2 as the most important DOR subtype modulating peripheral nociception (Tseng et al., 1994; Negri et al., 1995) further emphasizes the potential physiological relevance of our results.

As in previous work, the commonly used DOR-1 agonist DPDPE was ineffective (Schroeder et al., 1991; Moises et al., 1994; Liu et al., 1995). Because this compound inhibits HVACC currents in nonsensory neurons and non-neuronal cells (Motin et al., 1995; Nah et al., 1997; Toselli et al., 1997), DORs-1 could be implicated in such cases. However, a potential involvement of DORs-2 cannot as yet be dismissed because some cross-reactivity of DPDPE with DORs-2 has been recognized *in vivo* and *in vitro* (Vanderah et al., 1994; Wang et al., 1996; Toll et al., 1997). The involvement of an untested DOR subtype could explain why other studies in sensory neurons missed the δ opioid modulation of Ca^{2+} currents (Schroeder et al., 1991; Moises et al., 1994; Liu et al., 1995), although the age of experimental subjects (5- to 11-d-old here vs 21-d-old or older in other studies) and the overall low frequency of DOR-responding cells might have contributed as well.

In contrast to DORs, MORs seem neither necessary nor sufficient for the inhibition of the HVACC current by DADLE. The response occurred normally after the irreversible block of MORs, whereas it was completely blocked in the presence of an antagonist highly specific for DOR. The observed DADLE effect does require receptors other than MORs because cells showing a robust MOR-induced inhibition of the HVACC current did not respond to DADLE. Conversely, DADLE, but not an MOR agonist, inhibited K^+ and Ca^{2+} currents in single neurons expressing both DORs and MORs (Moore et al., 1994; Motin et al., 1995). Other significant differences distinguish the DOR-mediated DADLE effect from the HVACC current inhibition attributable to MORs (Schroeder et al., 1991; Rusin and Moises, 1995). First, only DADLE inhibited L-type currents. Second, the MOR response does not desensitize, whereas we and others found that the DOR-mediated DADLE response does (McFadzean and Docherty, 1989; Motin et al., 1995). Third, MORs inhibit the HVACC current in 90% of sensory neurons, whereas a substantially smaller overall proportion responds to DADLE (37%).

DORs-2 appear to be the only receptors that could by themselves mediate the inhibitory effect of the enkephalin analog on the HVACC current. However, it is important to note that the data are certainly compatible with a collective participation of more than one receptor in the production of the final cellular response. This seems indeed a reasonable expectation in view of the fact that DADLE, as well as the natural enkephalins, can interact with DORs-1, DORs-2, and MORs (Goldstein and Naidu, 1989; Negri et al., 1995). Testing this hypothesis will require a detailed study of the effect of different combinations and doses of selective opioid agonists on the various HVACC currents.

DOR-mediated inhibition of multiple HVACC current types

A major conclusion of this study is that DORs inhibit basically all pharmacological components (L, N, P, Q) of the HVACC current of immature postnatal sensory neurons, with the sole exception of the R fraction. A similar pattern has been reported for MORs (Schroeder et al., 1991; Rusin and Moises, 1995) and KORs

(Wiley et al., 1997), although those receptors do not target L-type currents. In addition, we report here for the first time the inhibition of neuronal P-currents by DORs. Our data are consistent with results obtained in neuroblastoma (Morikawa et al., 1995; Toselli et al., 1997) and chromaffin (Kleppisch et al., 1992; Albillos et al., 1996) cells. From the diversity of HVACC targets, DORs can be expected to activate membrane-delimited pathways leading to non-L-type channel inhibition by G-protein $\beta\gamma$ subunits (Walker and DeWaard, 1998) and also to generate cytosolic messengers implicated in L-type current modulation (Mathie et al., 1992; Cardenas et al., 1997). This complex machinery mediating DOR effects is only partially understood (Hescheler et al., 1987; Taussig et al., 1992; Laugwitz et al., 1993; Piros et al., 1996).

N-, P-, and Q-type HVACC were implicated in transmitter release in sensory neurons (Yu et al., 1992; Gruner and Silva, 1994) and brain (Reuter, 1996). If the modulation demonstrated here in neurite-free cells also takes place in nerve endings, then our data could account for the presynaptic inhibitory effects of δ opioids on the conduction of nociceptive impulses in the spinal cord and brain (Jessell and Iversen, 1977; Dickenson et al., 1987; Collin et al., 1991; Glaum et al., 1994; Wang et al., 1996; Zachariou and Goldstein, 1996). In this respect, anatomical work has clearly shown that DORs are located in presynaptic terminals of spinal cord-projecting neurons (Cheng et al., 1995; van Bockstaele et al., 1997) and thus optimally placed to modulate synaptic Ca^{2+} influx.

As a rule, neurotransmitters never completely inhibit Ca^{2+} currents, although the degree of inhibition may vary widely depending on the channel's phosphorylation state, isoforms, constituent subunits, and interaction with G-proteins (Swartz, 1993; Zhang et al., 1996; Zamponi, 1997; Roche and Treistman, 1998; Walker and DeWaard, 1998). In consonance with such an empirical "rule," DADLE only partially inhibits the L-, N-, and Q-type components. The P current, in contrast, appeared to be fully inhibited in most cells (Fig. 7*C*,*D*), a result that suggested a more effective functional coupling between DORs and those channels. Neither the imperfect selectivity of ω-Aga-IVA nor the limited precision of our quantitative measurements could entirely account for this finding, which was also reflected, in an independent manner, by the comparatively larger average P-type fraction in I_D. Thus, whereas L, N, and Q proportions in I_D and I_{Ba} closely agreed (18:18, 50:48, and 19:16, respectively), the P fraction in I_D almost doubled its fraction in I_{Ba} (26:14).

The ability of inhibiting L currents singles out DORs from most receptors because non-L-type current modulation is quite common, whereas L-type currents are rarely targeted in all neuronal types so far examined (Zhu and Ikeda, 1993; Amico et al., 1995; Boehm and Huck, 1996; Foehring, 1996; Viana and Hille, 1996). Interestingly, DOR-induced inhibition of L-type HVACC is found elsewhere only in secretory cells in which those channels mediate the Ca^{2+} influx needed for exocytosis (pituitary: Lightman et al., 1982; Al Zein et al., 1984; GH3: Piros et al., 1996; chromaffin: Kleppisch et al., 1992; Albillos et al., 1996). Our data and the evidence of Ca^{2+}-dependent exocytosis of substance P from sensory neuron somata (Huang and Neher, 1996) raise the interesting possibility, even if highly speculative, that a mechanism of DOR-modulated secretion involving L-type HVACC might be conserved across neuronal and non-neuronal cells. DOR modulation of somatic Ca^{2+} influx, via L- or non-L-type HVACC, could also potentially affect Ca^{2+}-dependent gene expression and neuron development (Murphy et al., 1991; Finkbeiner and Greenberg, 1996; Hardingham et al., 1997).

One should expect DORs to affect the transmission of diverse sensory modalities as a result of targeting various subpopulations of DRG neurons (Perl, 1992). Conduction along P-neurons might be particularly affected as they are preferentially targeted. From their size and substance P content, they could be grouped with nociceptive, slow-conducting neurons (Harper and Lawson, 1985; Cardenas et al., 1995; Gilabert and McNaughton, 1997). However, their unmistakable morphology has not been noted previously, and thus they are likely to represent a separate, novel subpopulation.

REFERENCES

Albillos A, Carbone E, Gandia L, Garcia A, Pollo A (1996) Opioid inhibition of Ca^{2+} channel subtypes in bovine chromaffin cells: selectivity of action and voltage-dependence. Eur J Neurosci 8:1561–1570.

Al Zein M, Lutz-Bucher B, Koch B (1984) Modulation by leu-enkephalin of peptide release from perifused neurointermediate pituitary. I. Selective effect on potassium-, veratridine- and isoproterenol-stimulated secretion of vasopressin. Neuroendocrinology 39:392–396.

Amico C, Marchetti C, Nobile M, Usai C (1995) Pharmacological types of calcium channels and their modulation by baclofen in cerebellar granules. J Neurosci 15:2839–2848.

Aronin N, DiFiglia M, Liotta AS, Martin JB (1981) Ultarstructural localization and biochemical features of immunoreactive leu-enkephalin in monkey dorsal horn. J Neurosci 1:561–577.

Bean BP (1989) Neurotransmitter inhibition of neuronal calcium currents by changes in channel voltage dependence. Nature 340:153–156.

Bilsky EJ, Wang T, Lai J, Porreca F (1996) Selective blockade of peripheral δ opioid agonist induced antinociception by intrathecal administration of δ receptor antisense oligodeoxynucleotide. Neurosci Lett 220:155–158.

Boehm S, Huck S (1996) Inhibition of N-type calcium channels: the only mechanism by which presynaptic α 2-autoreceptors control sympathetic transmitter release. Eur J Neurosci 8:1924–1931.

Bot NGF, Blake AD, Li S, Reisine T (1997) Opioid regulation of the mouse δ-opioid receptor expressed in human embryonic kidney 293 cells. Mol Pharmacol 52:272–281.

Buzas B, Toth G, Cavagnero S, Hruby VJ, Borsodi A (1992) Synthesis and binding characteristics of the highly δ-specific new tritiated opioid peptide, [3H]deltorphin II. Life Sci 50:75–78.

Cáceres A, Mautino J, Kosik K (1992) Supression of MAP-2 in cultured cerebellar macroneurons inhibits minor neurite formation. Neuron 9:607–618.

Carbone E, Swandulla D (1989) Neuronal calcium channels: kinetics, blockade and modulation. Prog Biophys Mol Biol 54:31–58.

Cardenas CG, Del Mar LP, Scroggs RS (1995) Variation in serotonergic inhibition of calcium channel currents in four types of rat sensory neurons differentiated by membrane properties. J Neurophysiol 74:1870–1879.

Cardenas CG, Del Mar LP, Scroggs RS (1997) Two parallel signaling pathways couple $5HT_{AA}$ receptors to N- and L-type calcium channels in C-like rat dorsal root ganglion cells. J Neurophysiol 77:3284–3296.

Cheng PY, Svingos AL, Wang H, Clarke CL, Jenab S, Beczkowska IW, Inturrisi CE, Pickel VM (1995) Ultrastructural immunolabeling shows prominent presynaptic vesicular localization of δ-opioid receptor within both enkephalin- and nonenkephalin-containing axon terminals in the superficial layers of the rat cervical spinal cord. J Neurosci 15:5976–5988.

Collin E, Mauborgne A, Burgoin S, Chantrel D, Hamon M, Cesselin F (1991) *In vivo* tonic inhibition of spinal substance P (-like material) release by endogenous opioid(s) acting at δ receptors. Neuroscience 44:725–731.

Dickenson AH, Sullivan AF, Knox R, Zajac JM, Roques BP (1987) Opioid receptor subtypes in the rat spinal cord: electrophysiological studies with μ- and δ-opioid receptor agonists in the control of nociception. Brain Res 413:36–44.

Erspamer V, Melchiorri P, Falconieri-Erspamer G, Negri L, Corsi R, Severini C, Barra D, Simmaco M, Kreil G (1989) Deltorphins: a family of naturally occurring peptides with high affinity and selectivity for δ opioid binding sites. Proc Natl Acad Sci USA 86:5188–5192.

Finkbeiner S, Greenberg ME (1996) Ca^{2+}-dependent routes to Ras: mechanisms for neuronal survival, differentiation, and plasticity? Neuron 16:233–236.

Foehring RC (1996) Serotonin modulates N- and P-type calcium currents in neocortical pyramidal neurons via a membrane-delimited pathway. J Neurophysiol 75:648–659.

Fox AP, Nowycky MC, Tsien RW (1987) Single-channel recordings of three types of calcium channels in chick sensory neurones. J Physiol (Lond) 394:173–200.

Gilabert R, McNaughton P (1997) Enrichment of the fraction of nociceptive neurones in cultures of primary sensory neurons. J Neurosci Methods 71:191–198.

Glaum SR, Miller RJ, Hammond DL (1994) Inhibitory actions of δ1-, δ2-, and μ-opioid agonists on excitatory transmission in lamina II neurons of adult rat spinal cord. J Neurosci 14:4965–4971.

Goldstein A, Naidu A (1989) Multiple opioid receptors: ligand selectivity profiles and binding site signatures. Mol Pharmacol 36:260–272.

Gruner W, Silva LR (1994) ω-Conotoxin sensitivity and presynaptic inhibition of glutamatergic sensory neurotransmission *in vitro*. J Neurosci 14:2800–2808.

Hamill OP, Marty A, Neher E, Sakmann B, Sigworth FJ (1981) Improved patch-clamp techniques for high-resolution current recording from cells and cell-free membrane patches. Pflügers Arch 39:85–100.

Hardingham G, Chawla S, Johnson C, Bading H (1997) Distinct functions of nuclear and cytoplasmic calcium in the control of gene expression. Nature 385:260–265.

Harper AA, Lawson SN (1985) Conduction velocity is related to morphological cell type in rat dorsal root ganglion neurones. J Physiol (Lond) 359:31–46.

Hayes AG, Sheehan MJ, Tyers MB (1985) Determination of the receptor selectivity of opioid agonist in the guinea pig ileum and mouse vas deferens by use of β-funaltrexamine. Br J Pharmacol 86:899–904.

Hell JW, Westenbroek RE, Warner C, Ahlijanian MK, Prystay W, Gilbert MM, Snutch TP, Catterall WA (1993) Identification and different subcellular localization of the neuronal class C and class D L-type calcium channel α_1 subunits. J Cell Biol 123:949–962.

Hescheler J, Rosenthal W, Trautwein W, Schultz G (1987) The GTP-binding protein, G_O, regulates neuronal calcium channels. Nature 325:445–447.

Hillyard DR, Monje VD, Mintz IM, Bean BP, Nadasdi L, Ramachandran J, Miljanich G, Azimi-Zoonooz A, McIntosh JM, Cruz LJ (1992) A new Conus peptide ligand for mammalian presynaptic Ca^{2+} channels. Neuron 9:69–77.

Huang L-YM, Neher E (1996) Ca^{2+}-dependent exocytosis in the somata of dorsal root ganglion neurons. Neuron 17:135–145.

Jessell TM, Iversen LL (1977) Opiate analgesics inhibit substance P release from rat trigeminal nucleus. Nature 268:549–551.

Ji RR, Zhang Q, Law PY, Low H, Elde R, Hökfelt T (1995) Expression of μ-, δ-, and κ-opioid receptor-like immunoreactivities in rat dorsal root ganglia after carrageenan-induced inflammation. J Neurosci 15:8156–8166.

Kasai H (1992) Volatge and time dependent inhibition of neuronal calcium channels by a GTP-binding protein in a mammalian cell line. J Physiol (Lond) 448:189–209.

Kieffer BL, Befort K, Gaveriaux-Ruff C, Hirth CG (1992) The δ-opioid receptor: isolation of a cDNA by expression cloning and pharmacological characterization. Proc Natl Acad Sci USA 89:12048–12052.

Kleppisch T, Ahnert-Hilger G, Gollasch M, Spicher K, Hescheler J, Schultz G, Rosenthal W (1992) Inhibition of voltage-dependent Ca^{2+} channels via α_2-adrenergic and opioid receptors in cultured bovine adrenal chromaffin cells. Pflügers Arch 421:131–137.

Kostyuk PG, Shuba MY, Savchenko AN (1988) Three types of calcium channels in the membrane of mouse sensory neurons. Pflügers Arch 411:661–669.

Laugwitz KL, Offermanns S, Spicher K, Schultz NGF (1993) μ and δ opioid receptors differentially couple to G protein subtypes in membranes of human neuroblastoma SH-SY5Y cells. Neuron 10:233–242.

Levine JD, Fields HL, Basbaum AI (1993) Peptides and the primary afferent nociceptor. J Neurosci 13:2272–2286.

Lightman SL, Iversen LL, Forsling ML (1982) Dopamine and [D-Ala2, D-Leu5]enkephalin inhibit the electrically stimulated neurohypophyseal release of vasopressin *in vitro*: evidence for calcium-dependent opiate action. J Neurosci 2:78–81.

Liu NJ, Xu T, Xu C, Li CQ, Yu YX, Kang HG, Han JS (1995) Cholecystokinin octapeptide reverses μ-opioid-receptor-mediated inhibition of calcium current in rat dorsal root ganglion neurons. J Pharmacol Exp Ther 275:1293–1299.

Llinás R, Sugimori M, Lin J, Cherksey B (1989) Blocking and isolation of a calcium channel from neurons in mammals and cephalopods utilizing a toxin fraction (FTX) from funnel-web spider poison. Proc Natl Acad Sci USA 86:1689–1693.

López HS, Brown AM (1991) Correlation between G protein activation and reblocking kinetics of Ca^{2+} channel currents in rat sensory neurons. Neuron 7:1061–1068.

Mathie A, Bernheim L, Hille B (1992) Inhibition of N- and L-type calcium channels by muscarinic receptor activation in rat sympathetic neurons. Neuron 8:907–914.

Mattia A, Farmer S, Takemori A, Sultana M, Portoghese P, Mosberg H, Bowen W, Porreca F (1992) Spinal opioid δ antinociception in the mouse: mediation by 5′- NTII-sensitive δ receptor subtype. J Pharmacol Exp Ther 260:518–525.

McDonough S, Swartz K, Mintz IM, Boland LM, Bean BP (1996) Inhibition of calcium channels in rat central and peripheral neurons by ω-conotoxin MVIIC. J Neurosci 16:2612–2623.

McFadzean I, Docherty RJ (1989) Noradrenaline- and enkephalin-induced inhibition of voltage-sensitive calcium currents in NG108–15 hybrid cells. Eur J Neurosci 1:141–147.

Miller KE, Seybold VS (1989) Comparison of met-enkephalin, dynorphin A, and neurotensin immunoreactive neurons in the cat and rat spinal cords. II. Segmental differences in the marginal zone. J Comp Neurol 279:619–628.

Mintz IM, Bean BP (1993) GABAB receptor inhibition of P-type Ca^{2+} channels in central neurons. Neuron 10:889–898.

Mintz IM, Adams ME, Bean BP (1992) P-type calcium channels in rat central and peripheral neurons. Neuron 9:85–95.

Moises HC, Rusin KI, Macdonald RL (1994) μ and κ-opioid receptors selectively reduce the same transient components of high-threshold calcium current in rat dorsal root ganglion sensory neurons. J Neurosci 14:5903–5916.

Moore SD, Madamba SG, Scweitzer P, Siggins GR (1994) Voltage-dependent effects of opioids on hippocampal CA3 pyramidal neurons *in vitro*. J Neurosci 14:809–820.

Morikawa H, Fukuda K, Kato S, Mori K, Higashida H (1995) Coupling of the cloned μ-opioid receptor with the ω-conotoxin-sensitive Ca^{2+} current in NG108–15 cells. J Neurochem 65:1403–1406.

Motin LG, Bennet MR, Christie MJ (1995) Opioids acting on δ-receptors modulate Ca^{2+} currents in cultured postganglionic neurones of avian ciliary ganglia. Neurosci Lett 193:21–24.

Mulder AH, Wardeh G, Hogenboom F, Frankhuyzen AL (1984) κ- and δ-opioid receptor agonists differentially inhibit striatal dopamine and acetylcholine release. Nature 308:278–280.

Murphy T, Worley P, Baraban J (1991) L-type voltage-sensitive calcium channels mediate synaptic activation of immediate early genes. Neuron 7:625–635.

Nah SY, Unteustsch A, Bunzow JR, Cook SP, Beacham DW, Grandy DK (1997) μ and δ opioids but not κ opioid inhibit voltage-activated Ba^{2+} currents in neuronal F-11 cell. Brain Res 766:66–71.

Narita M, Tseng LF (1995) Stimulation of spinal δ-opioid receptors in mice selectively enhances the attenuation of δ-opioid receptor-mediated antinociception by antisense oligodeoxynucleotide. Eur J Pharmacol 284:185–189.

Negri L, Improta G, Lattanzi R, Potenza RL, Luchetti F, Melchiorri P (1995) Interaction between the μ-agonist dermorphin and the δ-agonist [D-Ala2, Glu4]deltorphin in supraspinal antinociception and δ-opioid receptor binding. Br J Pharmacol 116:2931–2938.

Patil PG, de Leon M, Reed RR, Dubel S, Snutch TP, Yue DT (1996) Elementary events underlying voltage dependent G-protein inhibition of N-type calcium channels. Biophys J 71:2509–2521.

Perl ER (1992) Function of dorsal root ganglion neurons: an overview. In: Sensory neurons: diversity, development, and plasticity (Scott SA, ed), pp 3–23. New York: Oxford UP.

Piros ET, Prather PL, Law PY, Evans CJ, Hales TG (1996) Voltage-dependent inhibition of Ca^{2+} channels in GH3 cells by cloned μ- and δ-opioid receptors. Mol Pharmacol 50:947–956.

Ramabandran K, Phil M, Bansinath M (1990) The role of endogenous opioid peptides in the regulation of pain. Crit Rev Neurobiol 6:13–32.

Randall A, Tsien RW (1995) Pharmacological dissection of multiple types of Ca^{2+} channel currents in rat cerebellar granule neurons. J Neurosci 15:2995–3012.

Raynor K, Kong H, Chen Y, Yasuda K, Yu L, Bell GI, Reisine T (1994) Pharmacological characterization of the cloned κ-, δ-, and μ-opioid receptors. Mol Pharmacol 45:330–334.

Regan LJ, Sah DW, Bean BP (1991) Ca^{2+} channels in rat central and

peripheral neurons: high-threshold current resistant to dihydropyridine blockers and ω-conotoxin. Neuron 6:269–280.
Reisine T (1995) Opiate receptors. Neuropharmacology 34:463–472.
Reuter H (1996) Diversity and function of presynaptic calcium channels in the brain. Curr Opin Neurobiol 6:331–337.
Roche JP, Treistman SN (1998) The Ca^{2+} channel β_3 subunit differentially modulates G-protein sensitivity of α_{1A} and α_{1B} Ca^{2+} channels. J Neurosci 18:878–886.
Rogers H, Hayes AG, Birch PJ, Traynor JR, Lawrence AJ (1990) The selectivity of the opioid antagonist, naltrindole, for δ-opioid receptors. J Pharm Pharmacol 42:358–359.
Ruit KG, Elliott JL, Osborne PA, Yan Q, Snider WD (1992) Selective dependence of mammalian dorsal root ganglion neurons on nerve growth factor during embryonic development. Neuron 8:573–587.
Rusin KI, Moises HC (1995) μ-Opioid receptor activation reduces multiple components of high-threshold calcium current in rat sensory neurons. J Neurosci 15:4315–4327.
Schroeder JE, Fischbach PS, Zheng D, McCleskey EW (1991) Activation of μ opioid receptors inhibits transient high- and low-threshold Ca^{2+} currents, but spares a sustained current. Neuron 6:13–20.
Scroggs R, Fox AP (1991) Distribution of dihydropyridine and ω-conotoxin-sensitive calcium currents in acutely isolated rat and frog sensory neuron somata: diameter-dependent L channel expression in frog. J Neurosci 11:1334–1346.
Shen K, Crain SM (1989) Dual opioid modulation of the action potential duration of mouse dorsal root ganglion neurons in culture. Brain Res 491:227–242.
Sofuoglu M, Portoghese P, Takemori A (1991) Differential antagonism of δ opioid agonists by naltrindole and its benzofuran analog (NTB) in mice: evidence for δ opioid receptor subtypes. J Pharmacol Exp Ther 257:676–680.
Standifer KM, Chien CC, Wahlestedt C, Brown GP, Pasternak GW (1994) Selective loss of δ opioid analgesia and binding by antisense oligodeoxynucleotides to a δ opioid receptor. Neuron 12:805–810.
Stewart PE, Hammond DL (1994) Activation of spinal δ-1 or δ-2 opioid receptors reduces carrageenan-induced hyperalgesia in the rat. J Pharmacol Exp Ther 268:701–708.
Swartz KJ (1993) Modulation of Ca^{2+} channels by protein kinase C in rat central and peripheral neurons: disruption of G-protein mediated inhibition. Neuron 11:305–320.
Takemori AE, Larson DL, Portoghese PS (1981) The irreversible narcotic antagonistic and reversible agonistic properties of the fumarate methyl ester derivative of naltrexone. Eur J Pharmacol 70:445–451.
Taussig R, Sanchez S, Rifo M, Gilman AG, Belardetti F (1992) Inhibition of the ω-conotoxin-sensitive calcium current by distinct G-proteins. Neuron 8:799–809.
Toll L, Polgar WE, Auh JS (1997) Characterization of the δ-opioid receptor found in SH-SY5Y neuroblastoma cells. Eur J Pharmacol 323:261–267.
Toselli M, Tosetti P, Taglietti V (1997) μ and δ opioid receptor activation inhibits ω-conotoxin-sensitive calcium channels in a voltage and time-dependent mode in the human neuroblastoma cell line SH-SY5Y. Pflügers Arch 433:587–596.
Tottene A, Moretti A, Pietrobon D (1996) Functional diversity of P-type and R-type calcium channels in rat cerebellar neurons. J Neurosci 16:6353–6363.
Tseng LF, Collins KA, Kampine JP (1994) Antisense oligodeoxynucleotide to a δ-opioid receptor selectively blocks the spinal antinociception induced by δ-, but not μ- or κ-opioid receptor agonists in mouse. Eur J Pharmacol 258:R1–R3.
Tsunoo A, Yoshii M, Narahashi T (1986) Block of calcium channels by enkephalin and somatostatin in neuroblastoma-glioma hybrid NG108–15 cells. Proc Natl Acad Sci USA 83:9832–9836.
Van Bockstaele EJ, Commons K, Pickel VM (1997) δ-Opioid receptor in presynaptic axon terminals in the rat nucleus locus coeruleus: relationships with methionine5-enkephalin. J Comp Neurol 338:575–586.
Vanderah T, Takemori AE, Sultana M, Portoghese PS, Mosberg HI, Hruby VJ, Haaseth RC, Matsunaga TO, Porreca F (1994) Interaction of [D-Pen2, D-Pen5] enkephalin and [D-Ala2, Glu4] deltorphin with δ-opioid receptor subtypes *in vivo*. Eur J Pharmacol 252:133–137.
Viana F, Hille B (1996) Modulation of high voltage-activated calcium channels by somatostatin in acutely isolated rat amygdaloid neurons. J Neurosci 16:6000–6011.
Walker D, De Waard M (1998) Subunit interaction sites in voltage dependent calcium channels: role in channel function. Trends Neurosci 21:148–154.
Wang XM, Yan JQ, Zhang KM, Mokha SS (1996) Role of opioid receptors (μ, δ1, δ2) in modulating responses of nociceptive neurons in the superficial and deeper dorsal horn of the medulla (trigeminal nucleus caudalis) in the rat. Brain Res 739:235–243.
Wiley J, Moises HC, Gross RA, MacDonald RL (1997) Dynorphin A-mediated reduction in multiple calcium currents involves a Goα-subtype G protein in rat primary afferent neurons. J Neurophysiol 77:1338–1348.
Williams ME, Feldman DH, McCue AF, Brenner R, Velicelebi NGF, Ellis SB, Harpold MM (1992) Struture and functional expression of α-1, α-2 and β subunits of novel human neuronal calcium channel subtype. Neuron 8:71–84.
Xu H, Lu YF, Partilla JS, Pinto J, Calderon SN, Matecka D, Rice KC, Lai J, Porreca F, Ananthan S, Rothman RB (1998) Opioid peptide receptor studies. 8. One of the mouse brain δNCX binding sites is similar to the cloned mouse opioid δ receptor: further evidence for heterogeneity of δ opioid receptors. Peptides 19:343–350.
Yu C, Lin PX, Fitzgerald S, Nelson P (1992) Heterogeneous calcium currents and transmitter release in cultured mouse spinal cord and dorsal root ganglion neurons. J Neurophysiol 67:561–575.
Zachariou V, Goldstein BD (1996) δ-Opioid receptor modulation of the release of substance P-like immunoreactivity in the dorsal horn of the rat following mechanical or thermal noxious stimulation. Brain Res 736:305–314.
Zamponi GW, Bourinet E, Nelson D, Nargeot J, Snutch T (1997) Crosstalk between G proteins and protein kinase C mediated by the calcium channel α1 subunit. Nature 385:442–446.
Zhang JF, Ellinor PT, Aldrich RW, Tsien RW (1996) Multiple structural elements in voltage-dependent Ca^{2+} channels support their inhibition by G proteins. Neuron 17:991–1003.
Zhu Y, Ikeda SR (1993) Adenosine modulates voltage-gated Ca^{2+} channels in adult rat sympathetic neurons. J Neurophysiol 70:610–620.